Tetrahedron 68 (2012) 6569–6574

Contents lists available at SciVerse ScienceDirect

Tetrahedron

journal homepage: www.elsevier.com/locate/tet

Synthesis and two-photon absorption properties of multi-branched styryl derivatives containing π-bond and σ-electron pair as bridge based on 1,3,5-triazine

Zheng Zheng [a], Hong-ping Zhou [a,*], Guo-yi Xu [a], Zhi-peng Yu [a], Xiao-fei Yang [a], Long-huai Cheng [a], Lin Kong [a], Yan Feng [a], Jie-ying Wu [a], Yu-peng Tian [a,b,c]

[a] Department of Chemistry, Anhui University and Key Laboratory of Functional Inorganic Materials Chemistry of Anhui Province, 230039 Hefei, PR China
[b] State Key Laboratory of Crystal Materials, Shandong University, 250100 Jinan, PR China
[c] State Key Laboratory of Coordination Chemistry, Nanjing University, 210093 Nanjing, PR China

ARTICLE INFO

Article history:
Received 15 March 2012
Received in revised form 8 May 2012
Accepted 15 May 2012
Available online 29 May 2012

Keywords:
Triazine derivatives
Photophysical properties
Intra-molecular charge transfer
2PA cross section
σ-Electron pair as bridge

ABSTRACT

A series of new one, two, and three-branched two-photon absorption triazine derivatives with a π-bond and a σ-electron pair as a bridge have been synthesized and their photophysical properties have been systematically investigated. These chromophores showed obvious solvatochromic effects, i.e., significant bathochromic shifting of the emission spectra and larger Stokes shifts were observed in more polar solvents mainly due to intra-molecular charge transfer (ICT). The two-photon absorption (2PA) cross-section values were determined by the two-photon excited fluorescence (TPEF) measurements in DMF. This result further proved that a σ-electron pair as a bridge is an efficient way to transfer charge as well as a π bridge, and that their 2PA cross-section values (δ) increase with increasing branch number.

1. Introduction

Two-photon absorption (2PA) is a third-order non-linear optical process involving simultaneous absorption of two photons to reach the excited state. Fluorescent molecules with large 2PA cross-sections have attracted a great deal of attention due to their superior photophysical properties and various applications in 3D optical data storage, bioimaging, optical limiting, photodynamic therapy, and microfabrication.[1] Most of these applications are based on the fluorescence properties of the two-photon excited molecule. So the significant issue is how to synthesize the materials with large 2PA cross section. There are several efficient design strategies put forward to enhance the 2PA cross section of the molecular, such as the π-conjugated was employed to connect donor and acceptor symmetrically or asymmetrically to form D–A–D, D–π–A, D–π–D, D–π–A structures, macrocycles, dendrimers, polymers, and multi-branched molecules. Furthermore, several other studies on structure–property relationship reveal that the 2PA cross section increase with the D/A strength, chain length, and planarity of the π-center.[2] For the multi-branched molecules, which can significantly enhance 2PA cross sections because of the increase of chromophore density and the cooperative enhancement effect among the chromophores.

Previous studies show that many octupolar compounds based on a triazine core and electron-donating substituents have been reported to exhibit large 2PA cross-sections.[3] 1,3,5-Triazine-based compounds show good optical and electrical properties due to their high electron affinity and symmetrical structure.[4] Structurally, *N*,*N*-diethylaniline can enhance the extent of electron delocalization and ability to donate electrons of the 2PA compound. Until now, most of the studies about the two-photon materials employed C=C bonds as the linkage to combine a 1,3,5-triazine core with an electron-donating end group while little attention has been paid to the alteration of the acceptor–donor linkage. Recently, spectral, and photophysical characteristics of some *N*-triazinyl derivatives have been reported,[5] but 2PA and applications of such materials are studied rarely. Wang et al.[6] reported a new 2PA-active compound employing a nitrogen atom as the linkage to combine a 1,3,5-triazine core with styrylpyridyl groups. A σ-electron pair as a bridge can be used to not only extend the molecular conjugated system and promote solubility, but also to avoid the aggregation-induced fluorescence quenching of the strong π–π stacking

* Corresponding author. Tel.: +86 551 5108151; fax: +86 551 5107342; e-mail address: zhpzhp@263.net (H.p. Zhou).

0040-4020/$ – see front matter © 2012 Published by Elsevier Ltd.
doi:10.1016/j.tet.2012.05.050

interaction in these large flat π-systems. This motivates us to design a series of new compounds containing a 1,3,5-triazine unit and investigate their structure–property relationships.

In view of the above advantages we have strategically designed and presented a similar one-step method to prepare one-, two-branched compounds (**T1**, **T2**) and pull–push type octupolar triazine molecule (**T3**) by changing the ratio of RNH_2 and 2,4,6-trichloro-1,3,5-triazine. Their linear photophysical characterization was performed in different organic solvents and 2PA properties were investigated by means of two-photon fluorescence spectroscopy. Then their structure–property relations will be discussed on the molecular basis.

2. Results and discussion

2.1. Synthesis

Synthetic routes of these series of compounds **T1**–**T3** and their intermediates are depicted in Scheme 1. Diethylamine, 4-fluorobenzaldehyde, and cyanuric chloride are available commercially. The intermediate **1** and aldehyde **2** were synthesized efficiently according to the literature.[7,8] Compound **3** was produced by the Wittig reaction between the Wittig reagent and the corresponding aldehyde in the solid phase with *t*-BuOK as base.[9] Compound **4** was prepared by the hydrazine hydrate reduction method in the presence of Pd/C catalyst in ethanol medium.[10] The targeted compounds (**T1**–**T3**) were obtained by the palladium-catalyzed C–N coupling strategy.[11]

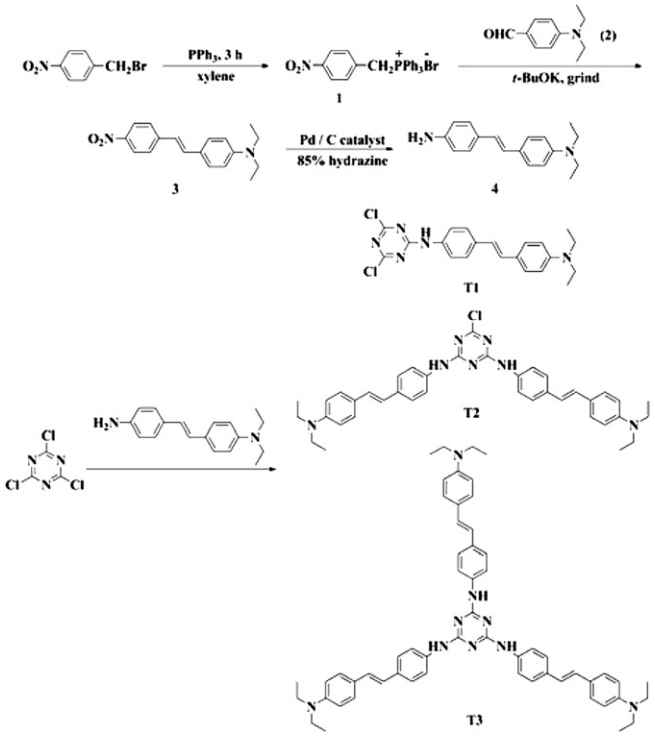

Scheme 1. Synthetic routes to target compounds **T1**–**T3**.

2.2. One-photon absorption and emission properties

The photophysical data of **T1**–**T3** are listed in Table 1. The one-photon absorption (OPA) and one-photon excited fluorescence (OPEF) were measured in five solvents of different polarities at a concentration $c=1\times10^{-5}$ mol L^{-1}. To further investigate the spectra relationship of the compounds, the one-photon absorption and the one-photon excited fluorescence data of **T1**–**T3** are restricted to DMF. Linear absorption and fluorescence spectra of **T1**–**T3** are shown in Figs. 1 and 2.

As shown in Fig. 1, compounds **T1**–**T3** exhibit one major absorption bands: the peak at about 370 nm is of charge-transfer character. The fluorescence deviation in solution can be attributed to the interaction of the solute with the local molecular environment including solvent molecules and other surrounding solute molecules. For each of the three compounds, the OPEF peak position λ_{max} showed an increasing tendency as the solvent polarity increased except in DMF. The Stokes shift also showed monotonically increasing tendency with the increase of solvent polarity except in DMF. On the other hand, the quantum yields (Φ) of **T1**–**T3** decreased consistently and significantly as the polarity of solvent increases except in DMF, and were especially highly quenched in acetonitrile (Fig. 1). These can be explained by the stronger solute/solvent interaction at the excited state comparing with that at the ground state, which indicates that the increasing polarity of the excited state increases. The energy level can be lowered greatly by increasing dipole–dipole interaction between the solute and solvent. However, a slight blue shift in absorption of **T1**–**T3** is observed in low polar solvents, while the absorption peaks are found to be red shifted in high polar solvents, such as acetonitrile and DMF. It may have great changes in the molecular geometry of excited states before fluorescence emission.

As listed in Table 1 and Fig. 2, from **T1** to **T3**, the one-photon absorption maxima in DMF show regular red shifts as the branch number increases and the spectral intensities also vary regularly, the absorption coefficients (ε_{max}) of the maxima increase consistently and significantly as the branch number increases. Note that the ε_{max} of **T1**–**T3** are of the order of 10^4 and they increase in the ratios 1.0:1.9:3.0 with the number of chromophores. These can be assigned to the extended π-delocalization and a certain coupling between the branches in **T2** and **T3**. The enhancement can be more clearly seen by revealing the reduced molar absorbance ε_{max}/MW, which is defined as ε_{max} divided by the molecular weight. The ε_{max}/MW values increase with a ratio of 1.0:1.2:1.4 for **T1**–**T3**. This means that the unit molecular weight leads to larger ε_{max} by incorporating more branches into the central triazine ring.

The OPEF maxima were obtained at their maxima excitation wavelengths in DMF. From **T1** to **T3**, OPEF spectra show slight blue shifts as the branch number increases. These blue shifts may be because *N*,*N*-diethylaniline serves as an electron donor, 1,3,5-triazine as an electron acceptor and styryl as a chromophore in these compounds. The ICT state of molecules with D–π–A structures has a high photoluminescence (PL) emission ability; hence, the single peak in the PL emission spectra manifests that the state responsible for the PL emission is not the localized excited state but the ICT state. Thus, the different dipole moments of the ICT state and the ground state lead to the shift in PL spectra.[3c] Note that the fluorescence quantum yields (Φ) of **T1**–**T3** reduce with the ratios of 3.8:2.6:1.0 as the branch number increases. This indicates that these chromophores employed the nitrogen atom as the linkage allowing internal rotation in the monomer form in organic solvents, whereby the fluorescence was reduced. This can be ascribed to the partial conjugation structure resulting from the delocalization of the lone pair electrons on nitrogen.

2.3. Two-photon properties

The two-photon excited fluorescence spectra (TPEF) of three compounds in DMF were recorded at their maximum excitation wavelength with a pulse duration of 140 fs under 500 mw (milliwatt). The TPEF data of **T1**–**T3** are described in Table 1 ($c=1\times10^{-3}$ mol L^{-1}).

Table 1
The linear and two-photon absorption properties of **T1**–**T3**

	Solvents	λ_{max}[a]	ε_{max}[b]	ε_{max}/MW[c]	λ_{max}[d]	$\Delta\nu$[e]	Φ[f]	λ_{max}[g]	σ[h]	σ/MW[i]
T1	Benzene	375	4.69		428	3302	0.138			
	THF	373	4.32		440	4082	0.096			
	Ethanol	370	4.40		442	4403	0.037			
	Acetonitrile	371	3.12		453	4879	0.013			
	DMF	**373**	**3.82**(**1.0**)	**0.0092**(**1.0**)	**453**	**4735**	**0.069**(**3.8**)	**481**	**1014**(**1.0**)	**2.45**(**1.0**)
T2	Benzene	376	7.75		428	3231	0.104			
	THF	373	8.75		442	4185	0.042			
	Ethanol	370	8.55		442	4403	0.016			
	Acetonitrile	370	4.83		454	5001	0.008			
	DMF	**375**	**7.26**(**1.9**)	**0.0113**(**1.2**)	**452**	**4543**	**0.047**(**2.6**)	**484**	**1810**(**1.8**)	**2.81**(**1.1**)
T3	Benzene	374	9.42		425	3209	0.100			
	THF	373	11.30		436	3874	0.063			
	Ethanol	364	7.86		440	4745	0.023			
	Acetonitrile	371	8.76		450	4732	0.014			
	DMF	**377**	**11.26**(**3.0**)	**0.0129**(**1.4**)	**451**	**4352**	**0.018**(**1.0**)	**488**	**2597**(**2.6**)	**2.97**(**1.2**)

[a] Absorption peak position in nm (1×10^{-5} mol L^{-1}).
[b] Maximum molar absorbance in 10^4 mol^{-1} L cm^{-1}.
[c] The reduced ε_{max}, i.e., the value of ε_{max} divided by the molecular weight, the numbers in parentheses are relative values by assigning that of **T1** as 1.
[d] Peak position of SPEF in nm (1.0×10^{-5} mol L^{-1}), excited at the absorption maximum.
[e] Stokes shift in cm^{-1}.
[f] Quantum yields determined by using coumarin 307 (1.0×10^{-5} mol L^{-1}) as the standard.
[g] TPEF peak position in nm pumped by femtosecond laser pulses at 500 mw at their maximum excitation wavelength.
[h] 2PA cross section in GM.
[i] Reduced cross section, i.e., 2PA cross section divided by molecular weight. The numbers in parentheses are relative values.

Two-photon fluorescence spectra of **T1**–**T3** in DMF pumped by femtosecond laser pulses under different pumped powers at their maximum excitation wavelengths are presented in Fig. 3a–c. The insets show logarithmic plots of the fluorescence integral versus pumped powers with a slope of 1.94, 1.96, and 1.96 when the input laser power is increasing, suggesting a two-photon excitation mechanism. As no linear absorption was observed in the range from 500 nm to 2000 nm, the emission excited by 730–740 nm laser wavelength can be attributed to the TPEF mechanism. As shown in Fig. 3d, all the three compounds display 2PA activity in the range of 680–780 nm in DMF.

It can be seen from Table 1 that the fluorescence peak wavelengths are obviously red-shifted by 28–37 nm compared to those of OPEF in DMF, which can be explained by the reabsorption effect. For one-photon induced emission measurements, we used dilute solutions (1×10^{-5} mol L^{-1}), thus the reabsorption of the fluorescence within the samples is negligible. In the case of two-photon excitation, concentrated solutions (1×10^{-3} mol L^{-1}) were used. Since the 730–740 nm laser beam can pass through the whole solution without linear depletion, the fluorescence emission is not only from the surface layer, but also from inside the solution sample. As a result, the reabsorption of the shorter wavelength fluorescence by the concentrated sample can no longer be neglected. The short wavelength side of the two-photon fluorescence was reabsorbed by the solution and red-shifts of the fluorescence spectra were readily observed.[12]

As shown in Fig. 4, the intensities of TPEF of **T1**–**T3** exhibit the sequence of **T3**<**T1**<**T2**. These similarities between TPEF and OPEF indicate that both the emissions for a given compound are from the

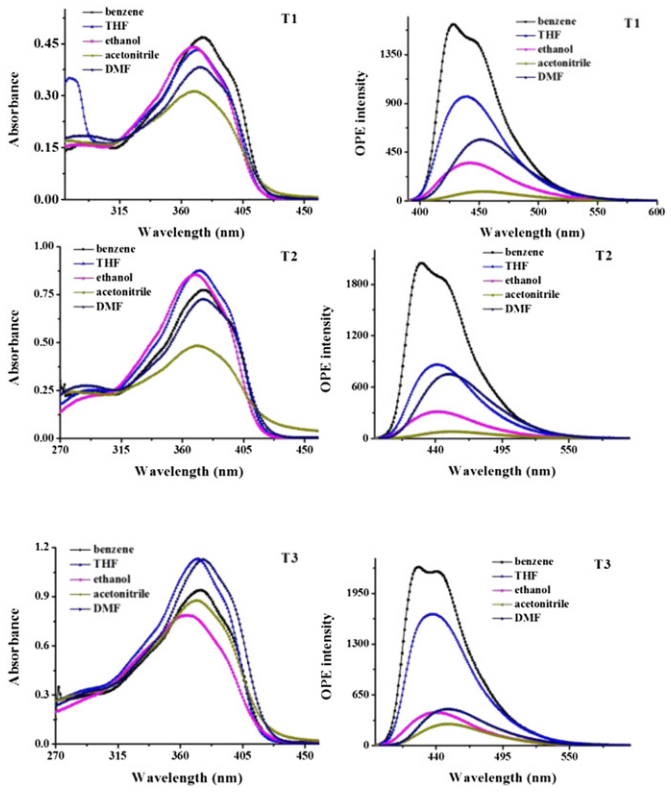

Fig. 1. Linear absorption and fluorescence of **T1**–**T3** in five organic solvents of different polarities with a concentration of 1×10^{-5} mol L^{-1}.

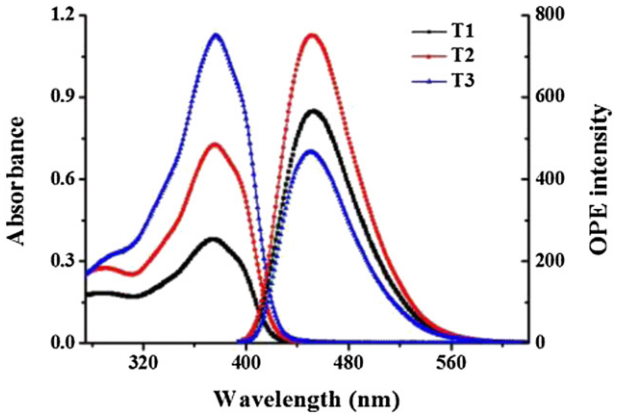

Fig. 2. OPA spectra (left) and OPEF spectra (right) of **T1**–**T3** in DMF with a concentration of 1×10^{-5} mol L^{-1}.

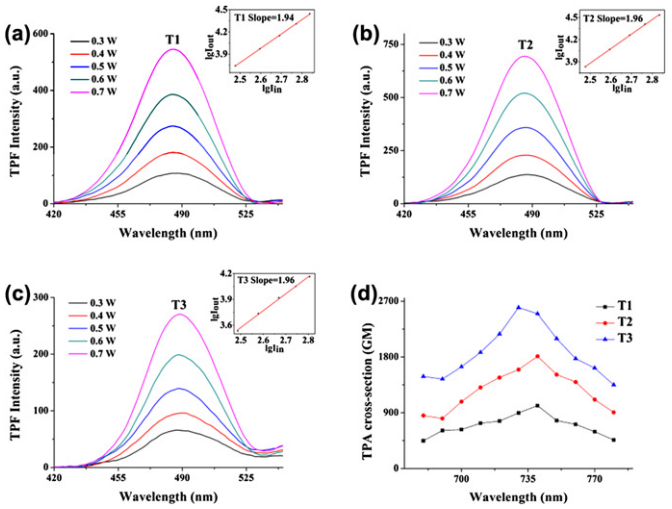

Fig. 3. (a)–(c) 2PF spectra of **T1**–**T3** in DMF pumped by femtosecond laser pulses under different pumped powers at their maximum excitation wavelength, insert contains the logarithmic plots of the fluorescence integral of chromophores versus different excitation intensities. (d) Two-photon absorption cross sections of **T1**–**T3** in DMF versus excitation wavelengths of identical energy of 0.5 w (experimental uncertainties: 10%).

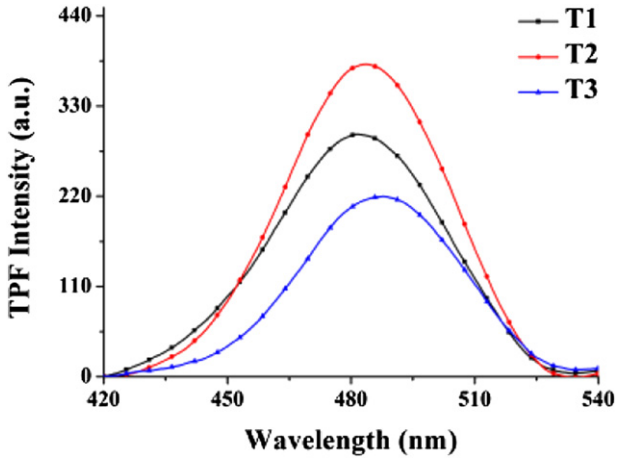

Fig. 4. The two-photon fluorescence spectra of **T1**–**T3** in DMF ($c=1\times10^{-3}$ mol L^{-1}) pumped by femtosecond laser pulses at 500 mw at their maximum excitation wavelength.

same excited state, though their initial Frank–Condon states may be different. The difference between TPEF and OPEF is mainly during the excitation process: two-photon absorption versus single-photon absorption. It can be seen from Table 1, the 2PA cross-section values (σ) increases obviously with the ratios of 1.0:1.8:2.6 as the branch number increases in the series of **T1**–**T3**. The reduced 2PA cross section σ/MW, which is defined as σ divided by the molecular weight, varies in a proportion of 1.0:1.1:1.2. This means that the unit molecular weight enables enhanced 2PA cross-section values as the branch number increases. This leads to the indication of some interactions between branches in the molecule, thus resulting in charge redistribution and extended delocalization. Consequently, the enhancement effect works in both linear and non-linear 2PA processes for compounds **T1**–**T3**.

With respect to our system, the nitrogen atom as the linkage was adopted to combine a 1,3,5-triazine core with substituents to provide a large 2PA cross sections (1014 GM, 1810 GM, 2597 GM), which indicates the lone pair electrons on the amino nitrogen atom of **T1**–**T3** may have delocalized onto the conjugated system of the molecule and it may increase intra-molecular charge transfer. Moreover, these well-conjugated structures allow sufficient electronic coupling between the branches, which has also been experimentally confirmed by the above-mentioned linear and nonlinear photophysical data.

3. Conclusion

We have reported one-step syntheses of a series of multi-branched two-photon absorbing triazine derivatives by changing the ratio of RNH_2 and 2,4,6-trichloro-1,3,5-triazine. The studies further demonstrated that having a σ-electron pair as bridge is an efficient way to transfer charge as well as a π bridge to induce a large 2PA cross section. Among the three compounds, **T3** was found to exhibit a large 2PA across section values (2597 GM) as measured by the two-photon induced fluorescence methods. We believe that the design method and fabrication strategy are potentially applicable to the derivatization of analogous two-photon absorption chromophores.

4. Experimental section

4.1. General experimental methods

Chemicals were purchased and used as received. Every solvent was purified as conventional methods beforehand. IR spectra were recorded with a Nicolet FT-IR NEXUS 870 spectrometer (KBr discs) in the 4000–400 cm^{-1} region. ^{1}H and ^{13}C NMR spectra were recorded on a 400 or 500 MHz NMR instrument using $CDCl_3$ or $(CD_3)_2CO$ as solvent. Chemical shifts were reported in parts per million (ppm) relative to internal TMS (0 ppm) and coupling constants in hertz. Splitting patterns were described as singlet (s), doublet (d), triplet (t), quartet (q), or multiplet (m). Mass spectra were obtained on a Micromass GCT-MS Spectrometer, and ESI-MS spectra were obtain on a Finnigan LCQ Spectrometer. MALDI-TOF mass spectra were recorded on a time-of-flight (TOF) mass spectrometer using a 337 nm nitrogen laser with alpha-cyano-4-hydroxycinnamic acid as matrix.

4.2. Optical measurements

The one-photon absorption (OPA) spectra were recorded on a UV-265 spectrophotometer. The one-photon excited fluorescence (OPEF) spectra measurements were performed using a Hitachi F-7000 fluorescence spectrophotometer. OPA and OPEF of **T1**–**T3** were measured in five organic solvents of different polarities with the concentration of 1.0×10^{-5} mol L^{-1}. The quartz cuvettes used are of 1 cm path length. The fluorescence quantum yields (Φ) were determined by using coumarin 307 as the reference according to the literature method.[13] Quantum yields were corrected as follows:

$$\Phi_s = \Phi_r\left(\frac{A_r\eta_s^2 D_s}{A_s\eta_r^2 D_r}\right)$$

where the s and r indices designate the sample and reference samples, respectively, A is the absorbance at λ_{exc}, η is the average refractive index of the appropriate solution, and D is the integrated area under the corrected emission spectrum.[14]

Two-photon absorption (2PA) cross-sections (δ) of the samples were obtained by two-photon excited fluorescence (TPEF) method[15] at femtosecond laser pulse and Ti: sapphire system (680–1080 nm, 80 MHz, 140 fs) as the light source. The sample was dissolved in different solvents at a concentration of 1.0×10^{-3} mol L^{-1}. The intensities of TPEF spectra of the reference and the sample were determined at their excitation wavelength. Thus, 2PA cross section (δ) of samples was determined by the equation:

$$\delta = \delta_{ref}\frac{\Phi_{ref}}{\Phi}\frac{c_{ref}}{c}\frac{n_{ref}}{n}\frac{F}{F_{ref}}$$

where the ref subscripts stand for the reference molecule (here fluorescein in aqueous solution at concentration of 1.0×10^{-3} mol L^{-1} was used as reference). δ is the 2PA cross-sectional value, c is the concentration of the solution, n is the refractive index of the solution, F is the TPEF integral intensities of the solution emitted at the exciting wavelength, and Φ is the fluorescence quantum yield. The δ_{ref} value of reference was taken from the literature.[16]

4.3. General procedure for the preparation of T1–T3

*4.3.1. 4-Nitro-benzyl-triphenylphosphonium bromide (**1**).* 4-Nitrobenzyl-triphenylphosphonium bromide was prepared referring the literature.[7]

*4.3.2. 4-Diethylaminobenzaldehyde (**2a**).* 4-Diethylaminobenzaldehyde was prepared referring the literature.[8]

*4.3.3. Preparation of **3**.* Compound **3** was prepared referring the literature.[9] 1.67 g **3** was obtained as a dark red flaky solid. Yield: 31.3%. Mp: 162–164 °C; IR (KBr, cm^{-1}) 2977, 2925, 1603, 1578, 1520, 1503, 1378, 1329, 1103, 969, 749, 687; ^{1}H NMR (400 Hz, $(CD_3)_2CO$) δ 8.19 (d, J=8.8 Hz, 2H), 7.75 (d, J=8.8 Hz, 2H), 7.50 (d, J=9.2 Hz, 2H), 7.41 (d, J=16.0 Hz, 1H), 7.08 (d, J=16.0 Hz, 1H), 6.73 (d, J=9.2 Hz, 2H), 3.45 (q, J=7.1 Hz, 4H), 1.17 (t, J=7.2 Hz, 6H); ^{13}C NMR (100 MHz, $CDCl_3$) δ 148.3, 145.8, 145.2, 133.8, 133.1, 132.2, 132.0, 131.94, 131.92, 128.7, 128.6, 128.4, 126.0, 124.2, 123.3, 120.9, 111.5, 44.4, 12.6; HRMS (GCT-MS): found 296.1505. $C_{18}H_{20}N_2O_2$ requires 296.1525.

*4.3.4. Preparation of **4**.* A solution of 1.85 g (6.2 mmol) of **3** dissolved in 40 mL ethanol was added into a round-bottom flask equipped with a magnetic stirrer and heated at 80 °C. Then 1.25 g of Pd/C catalyst was added into the preceding reaction system and a solution of 7.4 g of 85% hydrazine hydrate was added dropwise for about 0.5 h. The reaction was monitored by TLC. After the completion of the reaction, the mixture was filtered immediately, stirred by slowly adding appropriate amount of water and filtered under vacuum to give 1.35 g of white solid. Yield: 82.0%. Mp: 109–110 °C; IR (KBr, cm^{-1}) 3450, 3364, 3016, 2967, 2967, 1609, 1520, 1463, 1371, 1356, 1261, 1195, 1151, 962, 824; ^{1}H NMR (400 Hz, $(CD_3)_2CO$) δ 7.32 (d, J=8.4 Hz, 2H), 7.24 (d, J=8.4 Hz, 2H), 6.82 (s, 2H), 6.67 (d, J=8.8 Hz, 2H), 4.66 (s, 2H), 3.39 (q, J=7.1 Hz, 4H), 1.14 (t, J=7.2 Hz, 6H); ^{13}C NMR (125 MHz, $CDCl_3$) δ 147.0, 145.4, 129.4, 129.2, 127.5, 127.3, 125.6, 124.2, 115.5, 112.0, 44.7, 12.8; HRMS (GCT-MS): found 266.1777. $C_{18}H_{22}N_2$ requires 266.1783.

*4.3.5. Preparation of **T1**.* A suspension of 0.14 g (0.75 mmol) of cyanuric chloride, 0.22 g (1.5 mmol) of anhydrous K_2CO_3 dissolved in 5 mL of dry THF was added into a round-bottom flask equipped with a magnetic stirrer in the ice bath, and a solution of 0.2 g (0.75 mmol) of **4** dissolved in 10 mL dry THF was added dropwise and stirred at room temperature for 1 h. Then the mixture was refluxed at 70 °C for 8 h. The reaction was monitored by TLC. After the completion of the reaction, appropriate amount of CH_2Cl_2 was added with stirring and the solution was washed three times with water. The organic phase was obtained after removing the aqueous phase. Then it was dried with anhydrous $MgSO_4$, filtered, concentrated, and recrystallized with ethanol to give 0.15 g of yellow solid. Yield: 49.0%. Mp: >300 °C; IR (KBr, cm^{-1}) 3421, 3017, 2969, 2928, 1601, 1570, 1518, 1501, 1373, 1265, 1151, 1188, 1076, 961, 825, 797; ^{1}H NMR (400 Hz, $(CD_3)_2CO$) δ 9.91 (s, 1H), 7.71 (d, J=8.4 Hz, 2H), 7.58 (d, J=8.8 Hz, 2H), 7.43 (d, J=8.8 Hz, 2H), 7.13 (d, J=16.4 Hz, 1H), 6.96 (d, J=16.4 Hz, 1H), 6.71 (d, J=8.8 Hz, 2H), 3.43 (q, J=7.1 Hz, 4H), 1.16 (t, J=7.0 Hz, 6H); ^{13}C NMR (100 MHz, $CDCl_3$) δ 168.4, 164.2, 147.4, 137.1, 133.9, 128.2, 126.4, 124.5, 123.0, 121.8, 111.8, 44.1, 13.0; HRMS (GCT-MS): found 413.1177. $C_{21}H_{21}Cl_2N_5$ requires 413.1174.

*4.3.6. Preparation of **T2**.* A suspension of 0.14 g (0.75 mmol) of cyanuric chloride, 0.58 g (4.5 mmol) of DIPEA dissolved in 5 mL of dry THF was added into a round-bottom flask equipped with a magnetic stirrer in an ice-bath, and a solution of 0.2 g (0.75 mmol) of **4** dissolved in 10 mL dry THF was added dropwise and stirred at room temperature for 1 h. Then the reaction mixture was refluxed at 70 °C for 8 h. Another molar amount of **4** (0.2 g, 0.75 mmol) was added dropwise into the preceding reaction system. The reaction was refluxed and monitored by TLC. After the completion of the reaction, appropriate amount of CH_2Cl_2 was added and the solution was washed with water. The organic phase was dried with anhydrous $MgSO_4$, filtered, concentrated, and recrystallized with ethanol to give 0.13 g of yellow solid. Yield: 27.5%. Mp: >300 °C; IR (KBr, cm^{-1}) 3421, 3017, 2969, 2928, 1601, 1570, 1501, 1373, 1264, 1188, 1076, 960, 825, 797; ^{1}H NMR (400 Hz, $(CD_3)_2CO$) δ 9.09 (s, 2H), 7.75 (d, J=7.2 Hz, 4H), 7.53 (d, J=7.6 Hz, 4H), 7.41 (d, J=8.8 Hz, 4H), 7.15 (d, J=16.4 Hz, 2H), 6.93 (d, J=16.0 Hz, 2H), 6.72 (d, J=8.8 Hz, 4H), 3.43 (q, J=7.1 Hz, 8H), 1.17 (t, J=7.0 Hz, 12H); ^{13}C NMR (100 MHz, $CDCl_3$) δ 168.5, 164.2, 147.4, 137.2, 133.9, 128.2, 126.4, 124.5, 123.0, 121.8, 111.9, 44.1, 13.0; HRMS (MSI): found 644.5000. $C_{39}H_{43}ClN_7$ requires 644.3268.

*4.3.7. Preparation of **T3**.* A suspension of 0.057 g (0.31 mmol) of cyanuric chloride, 0.247 g (0.93 mmol) of intermediate **4**, 0.130 g (1.24 mmol) of anhydrous Na_2CO_3, and 30 mL of DMF under nitrogen was added into a three-necked flask equipped with a magnetic stirrer, a reflux condenser, and a nitrogen input tube. The reaction mixture was heated to 140 °C for 0.5 h and then 0.05 g (5 mol %) $Pd(PPh_3)_4$ was added. The reaction mixture was refluxed about 30 h and monitored by TLC. Then appropriate amount of CH_2Cl_2 was added and the solution was washed with water. The organic phase was dried with anhydrous $MgSO_4$, filtered, and concentrated. The gray product was purified by column chromatography with petroleum (bp 60–90 °C)/ethyl acetate (5:1 by volume) as eluent to yield 0.11 g of yellow solid. Yield: 41.4%. Mp: >300 °C; IR (KBr, cm^{-1}) 3390, 3018, 2968, 2927, 1603, 1519, 1488, 1412, 1374, 1265, 1186, 1076, 959, 823; ^{1}H NMR (400 Hz, $CDCl_3$) δ 7.56 (d, J=8.4 Hz, 6H), 7.44 (d, J=8.0 Hz, 6H), 7.40 (d, J=8.4 Hz, 6H), 7.50 (d, J=16.4 Hz, 3H), 6.90 (d, J=16.4 Hz, 3H), 6.68 (d, J=8.4 Hz, 6H), 3.40 (q, J=7.1 Hz, 12H), 1.20 (t, J=7.0 Hz, 18H); ^{13}C NMR (100 MHz, $CDCl_3$) δ 164.2, 147.2, 137.1, 133.5, 127.8, 127.7, 126.4, 125.1, 123.5, 120.9, 111.8, 44.4, 12.7; MALDI-TOF: found 873.4152. $C_{57}H_{63}N_9$ requires 873.5206.

Acknowledgements

This work was supported by Program for New Century Excellent Talents in University (China), Doctoral Program Foundation of Ministry of Education of China (20113401110004), Science and Technological Fund of Anhui Province for Outstanding Youth (10040606Y22), National Natural Science Foundation of China (21071001, 51142011, 21102001, and 21101001), Natural Science Foundation of Education Committee of Anhui Province (KJ2012A024, KJ2010A030), the 211 Project of Anhui University, the Team for Scientific Innovation Foundation of Anhui Province (2006KJ007TD), Ministry of Education Funded Projects Focus on Returned Overseas Scholar, and Anhui University Student Innovative Experiment Plan (XJ103575023, KYXL201100337). Thank Lingxia Zheng of Department of Physics and Materials Science of City University of Hong Kong for her help in writing the paper.

Supplementary data

Supplementary data associated with this article can be found in the online version, at doi:10.1016/j.tet.2012.03.055. These data include MOL files and InChiKeys of the most important compounds described in this article.

References and notes

1. (a) Yao, S.; Ahn, H. Y.; Wang, X. H.; Fu, J.; Stryland, E. W. V.; Hagan, D.; Belfield, K. D. *J. Org. Chem.* **2010**, *75*, 3965–3974; (b) Andrade, C. D.; Yanez, C. O.; Rodriguez, L.; Belfield, K. D. *J. Org. Chem.* **2010**, *75*, 3975–3982; (c) Dvornikov, A. S.; Walker, E. P.; Rentzepis, P. M. *J. Phys. Chem. A* **2009**, *113*, 13633–13644; (d) Tian, H.; Feng, Y. L. *J. Mater. Chem.* **2008**, *18*, 1617–1622; (e) Barsu, C.; Cheaib, R.; Chambert, S.; Queneau, Y.; Maury, O.; Cottet, D.; Wege, H.; Douady, J.; Bretonniere, Y.; Andraud, C. *Org. Biomol. Chem.* **2010**, *8*, 142–150; (f) Lin, T. C.; Haung, Y. J.; Chen, Y. F.; Hu, C. L. *Tetrahedron* **2010**, *66*, 1375–1382; (g) LaFratta, C. N.; Fourkas, J. T.; Baldacchini, T.; Farrer, R. A. *Angew. Chem., Int. Ed.* **2007**, *46*, 6238–6258; (h) Cumpston, B. H.; Ananthavel, S. P.; Barlow, S.; Dyer, D. L.; Ehrlich, J. E.; Erskine, L. L.; Heikal, A. A.; Kuebler, S. M.; Lee, I. Y. S.; McCord-Maughon, D.; Qin, J. Q.; Rockel, H.; Rumi, M.; Wu, X. L.; Marder, S. R.; Perry, J. W. *Nature* **1999**, *398*, 51–54.
2. Mongin, O.; Porrès, L.; Charlot, M.; Katan, C.; Blanchard-Desce, M. *Chem.—Eur. J.* **2007**, *13*, 1481–1498.
3. (a) Kannan, R.; He, G. S.; Lin, T. C.; Prasad, P. N.; Vaia, R. A.; Tan, L. S. *Chem. Mater.* **2004**, *16*, 185–194; (b) Cui, Y. Z.; Fang, Q.; Xue, G.; Xu, G. B.; Yin, L.; Yu, W. T. *Chem. Lett.* **2005**, *34*, 644–645; (c) Li, B.; Tong, R.; Zhu, R.; Meng, F.; Tian, H.; Qian, S. X. *J. Phys. Chem. B* **2005**, *109*, 10705–10710; (d) Wang, Y. C.; Jiang, Y. H.; Hua, J. L.; Tian, H.; Qian, S. X. *J. Appl. Phys.* **2011**, *110*, 033518-1-033518-10.
4. (a) Inomata, H.; Goushi, K.; Masuko, T.; Konno, T.; Imai, T.; Sasabe, H.; Brown, J. J.; Adachi, C. *Chem. Mater.* **2004**, *16*, 1285–1291; (b) Zhong, H.; Xu, E.; Zeng, D.; Du, J.; Sun, J.; Ren, S.; Jiang, B.; Fang, Q. *Org. Lett.* **2008**, *10*, 709–712; (c) Jiang, Y. H.; Wang, Y. C.; Wang, B.; Yang, J. B.; He, N. N.; Qian, S. X.; Hua, J. L. *Chem.—Asian J.* **2011**, *6*, 157–165.
5. (a) Murase, T.; Fujita, M. *J. Org. Chem.* **2005**, *70*, 9269–9278; (b) El-Sedik, M.; Almonasy, N.; Nepraš, M.; Bureš, F.; Dvořák, M.; Michl, M.; Čermák, J.; Hrdina, R. *Dyes Pigm.* **2012**, *92*, 1126–1131; (c) Nepraš, M.; Almonasy, N.; Michl, M.; Dvořák, M.; Fidler, V. *Dyes Pigm.* **2012**, *92*, 1331–1336.
6. Yan, Y. X.; Fan, H. H.; Guo, Y. H.; Lam, C. K.; Huang, H.; Sun, Y. H.; Tian, L.; Wang, C. K.; Tian, Y. P.; Wang, H. Z.; Chen, X. M. *Mater. Chem. Phys.* **2007**, *101*, 329–335.
7. Whittall, I. R.; Humphrey, M. G. *Organometallics* **1996**, *15*, 1935–1941.
8. (a) Hao, F. Y.; Zhang, X. J.; Tian, Y. P.; Zhou, H. P.; Li, L.; Wu, J. Y.; Zhang, S. Y.; Yang, J. X.; Jin, B. K.; Tao, X. T.; Zhou, G. Y.; Jiang, M. H. *J. Mater. Chem.* **2009**, *19*, 9163–9169; (b) Gan, X. P.; Zhou, H. P.; Shi, P. F.; Wang, P.; Wu, J. Y.; Tian, Y. P.; Yang, J. X.; Xu, G. B.; Zhou, Y. F.; Jiang, M. H. *Sci. China, Ser. B: Chem.* **2009**, *52*, 2180–2185.
9. Zhou, H. P.; Zhou, F. X.; Wu, P.; Zheng, Z.; Yu, Z. P.; Chen, Y. X.; Tu, Y. L.; Kong, L.; Wu, J. Y.; Tian, Y. P. *Dyes Pigm.* **2011**, *91*, 237–247.
10. Yang, C. P.; Chen, W. T. *Macromolecules* **1993**, *26*, 4865–4871.
11. (a) Almonasy, N.; Nepraš, M.; Hyková, Š.; Lyčka, A.; Čermák, J.; Dvořák, M.; Michl, M. *Dyes Pigm.* **2009**, *82*, 164–170; (b) Almonasy, N.; Nepraš, M.; Hyková, Š.; Lyčka, A.; Čermák, J.; Dvořák, M.; Michl, M. *Dyes Pigm.* **2009**, *82*, 416–421.
12. Xu, F.; Wang, Z. W.; Gong, Q. H. *Opt. Mater.* **2007**, *29*, 723–727.
13. Demas, J. N.; Crosby, G. A. *J. Phys. Chem.* **1971**, *75*, 991–1024.
14. Gray, T. G.; Rudzinski, C. M.; Meyer, E. E.; Holm, R. H.; Nocera, D. G. *J. Am. Chem. Soc.* **2003**, *125*, 4755–4770.
15. Lee, S. K.; Yang, W. J.; Choi, J. J.; Kim, C. H.; Jeon, S. J.; Cho, B. R. *Org. Lett.* **2005**, *7*, 323–326.
16. Xu, C.; Webb, W. W. *J. Opt. Soc. Am. B* **1996**, *13*, 481–491.